STRUCTURAL AND MAGNETIC PROPERTIES OF NANOMATERIALS PREPARED BY MODIFICATION OF IRON NANOPARTICLES AND THEIR EFFICIENCY IN Cr(VI) REMOVAL: A COMPARATIVE STUDY

Josef KAŠLÍK, Ivo MEDŘÍK, Jan FILIP, Eleni PETALA, Ondřej MALINA, Radek ZBOŘIL

Regional Centre of Advanced Technologies and Materials, Palacký University, Olomouc, Czech Republic, EU, josef.kaslik@upol.cz

Abstract

Technologies involving iron-based nanomaterials, such as nanoscale zero-valent iron (nZVI), are extensively used for elimination of various contaminants in the environment. In this study, we modified commercial nZVI particles NANOFER 25P (from NANO IRON company, CZ) via one-step thermal treatment under different conditions (including temperature, time, and atmosphere), in a way that has not been previously reported. The structural, magnetic and air-stability aspects of the as-prepared materials were investigated by means of X-ray powder diffraction, Mössbauer spectroscopy, and magnetic and surface area measurements. The characterization revealed that each of the materials is dominantly formed by different crystalline phase (i.e., iron nitrides Fe_4N and $Fe_{2.43}N$, FeO, and Fe_3C) and that the modification occurred in almost entire volume of the particles rather than only on the surface. Moreover, the as-prepared materials were evaluated for their efficiency of Cr(VI) removal and compared with bare nZVI used for their preparation.

Keywords: Solid state reaction, modification, iron nitride, iron carbide, characterization

1. INTRODUCTION

Nanoscale zero valent iron (nZVI) belongs to the group of widely studied materials with a great potential in various environmental applications. It can be effectively utilized in reductive remediation technologies for degradation of numerous inorganic and organic contaminants, including heavy metals, nitrates, chemical warfare agents, polychlorinated hydrocarbons, pesticides, organic dyes and antibiotics [1-3].

Although the high reactivity of bare nZVI is undoubtedly their great advantage, it also causes fast oxidation during their exposure to the air. Therefore such materials have to be stored and handled under inert conditions or in slurry which increase cost of the material. The other possibility is stabilization of the particles by creation of inorganic passivating shell on the particle surface, which can be formed either by iron oxide or by carbon and/or iron carbides [4,5]. Such shell protects the particles against further oxidation and the materials can therefore be stored and manipulated without special requirements.

In this paper, we present a different approach of nZVI modification. Four materials were prepared via one-step thermal treatment of bare nZVI in various conditions (namely temperature, time, composition and pressure of environment). The as-prepared materials were characterized from structural, magnetic and stability point of view. Moreover, their efficiency in Cr(VI) removal was evaluated.

2. EXPERIMENTAL SECTION

2.1. Materials preparation

All materials were synthesized via one step solid state-gas reaction using commercial nZVI NANOFER 25P (NANO IRON, CZ) as a precursor. The samples N1 and N2 were prepared by annealing of 35g of nZVI in a mixture of NH_3 and N_2 (in ratio 1:2) with relative overpressure 0.5 bar for 120 min at temperatures 200 and

250 °C, respectively. The samples W1 and C1 were prepared by annealing of 55 g of NANOFER 25P in the mixture of CO_2 and H_2 (ratio 4:1) and relative gas overpressure 0.25 bar at 580 °C for 300 min and 500 °C for 240 min, respectively. All prepared materials were cooled down to room temperature in the furnace, transported under inert conditions to the glove-box, and stored there prior use. The commercial nZVI NANOFER 25P (labeled as NF25) was used as a reference for evaluation of the efficiency of prepared materials for Cr(VI) removal.

2.2. Characterization techniques

X-ray powder diffraction was performed on X`Pert PRO MPD powder diffractometer (Malvern Panalytical) equipped with iron filtered Co$K_\alpha$ radiation source and fast X`Celerator detector. The samples were deposited (under nitrogen atmosphere) on zero background Si slide and covered with Mylar foil. The High Score Plus software in conjunction with PDF-4+ and ICSD databases were used for evaluation of captured data.

Transmission ^{57}Fe Mössbauer spectra were measured at room temperature employing a MS2007 Mössbauer spectrometer based on virtual instrumentation technique, using a constant acceleration drive spectrometer and a commercial ^{57}Co(Rh) radiation source. The acquired spectra were evaluated using the MossWinn software. The isomer shift values were referred to α-Fe foil at room temperature.

A superconducting quantum interference device (SQUID, MPMS XL-7, Quantum Design, USA) was used for the magnetization measurements. The hysteresis loop measurements were recorded at the temperature of 300 K and in external magnetic fields ranging from -5 to +5 T.

Specific surface area (SSA) was measured employing Autosorb iQ analyzer (Quantachrome) at temperature of liquid nitrogen (77.4 K). The materials were degassed before measurement at room temperature for 12 hours. SSA was calculated using the multipoint BET3 method in p/p_0 between 0.01 and 0.30. The analysis was performed with the AsiQwin software (Quantachrome).

2.3. Reactivity evaluation

The efficiency of the as-prepared materials towards Cr(VI) removal was evaluated under aerobic conditions. In a typical procedure, 10 mg of each sample were mixed with 100 mL of prepared solution with concentration of Cr(VI) 6.5 mg/L. The pH was adjusted to 5.5 by HCl and the bottle with solution was shaken on a rotational shaker at room temperature for 48 hours. After 48 hours, 0.3 mL of the Cr(VI) solution was withdrawn and used for colorimetric measurement. The Cr(VI) concentration was determined by the 1,5-diphenylcarbazide method, which is based on the reaction of Cr(VI) cations with 1,5-diphenylcarbazide molecules leading to the formation of a red−purple chromium 1,5-diphenylcarbazide complex that shows absorbance maximum at 541.5 nm. 0.3 mL of the Cr(VI) solution was mixed with 2.7 mL of distilled water, 120 µL of 1,5-diphenylcarbazide acetone solution (10.3 mM) and 60 µL of H_3PO_4 aqueous solution (0.86 M). The solution was left 10 min to allow color development, and then the concentration was determined by UV-Vis spectroscopy. A calibration curve (in the range 0 - 1 mg/L) has been previously determined.

3. RESULTS AND DISCUSSION

3.1. Structural and magnetic aspects of prepared materials

The structural and phase analysis revealed that each of the prepared samples is dominantly formed by different crystalline phase (see **Table 1** and **Figure 1**). The samples prepared in a mixture of ammonium with nitrogen are formed mostly by iron nitrides, namely Fe_4N for sample N1, and $Fe_{2.43}N$ for sample N2. The samples prepared in mixture of carbon dioxide with nitrogen are formed mostly by wüstite and iron carbide (samples W1, and C1, respectively). This indicates that the modification took place in almost full volume of the particles rather than just by creation of the surface shell on the particles. However, except sample W1, all other samples contained small amount of α-Fe (less than 11 wt%; for details see **Table 1**). Additionally, all samples

contained small amount of magnetite/maghemite (less than 12 wt%). When the temperature applied during thermal treatment was equal to 500 °C or higher (i.e., during preparation of the samples W1 and C1), then the silicon, which is the trace element contained in nZVI precursor, formed separate Fe_2SiO_4 phase (fayalite). Its content increased with increasing temperature (i.e., from 6 wt% for sample W1 to 10 wt% for sample C1). The crystallinity (i.e., the mean X-ray coherence length (MCL)) of the dominant phases increased with increasing temperature from 35 nm for Fe_4N in N1 sample to 119 nm for Fe_3C in C1 sample.

The SSA was measured for all prepared materials, and additionally for precursor NF_25. While the samples N1 and N2 keep the SSA similar to the precursor (17.9, 18.0, m^2/g for N1 and N2, respectively, compared to 17.8 m^2/g for NF_25), the SSA of samples W1 and C1 significantly drop to 7.3 and 6.2 m^2/g, respectively. Such decrease is presumably caused by the temperature induced sintering of the particles during preparation of the materials, being thus consistent with the evolution of MCL.

Table 1 Quantification of relative content (RC) of crystalline phases in prepared materials and their mean X-ray coherence lengths (MCL)

Sample	α-Fe		FeO		Fe_3O_4/ γ-Fe_2O_3		Fe_2SiO_4	Fe_3C		$Fe_{2.43}N$		Fe_4N	
	RC (wt%)	MCL (nm)	RC (wt%)	MCL (nm)	RC (wt%)	MCL (nm)	RC (wt%)	RC (wt%)	MCL (nm)	RC (wt%)	MCL (nm)	RC (wt%)	MCL (nm)
N1	11	44	---	---	12	31	---	---	---	2	35	75	35
N2	1	43	---	---	4	32	---	---	---	69	54	26	34
W1	---	---	94	58	<1	41	6	---	---	---	---	---	---
C1	3	80	2	33	<1	65	10	85	119	---	---	---	---

The Mössbauer spectra of all samples are quite complicated (see **Figure 1** and **Table 2**). For the both samples containing nitrides (i.e., N1 and N2), each spectrum composes of 7 components: one sextet (*S1*) can be ascribed to α-Fe, two sextets (*S2* and *S3*) to Fe atoms in nonstoichiometric magnetite (where sextet *S3* represents octahedral iron atoms with effective valence 2,5+ observed because of electron hopping effect; i.e., paired Fe^{2+} and Fe^{3+}; and sextet *S2* represents tetrahedral Fe^{3+} and unpaired octahedral Fe^{3+} ions) [6], three sextets (*S4*, *S5*, and *S6*) to Fe atoms with nonequivalent neighborhood in Fe_4N [7] and doublet (*D1*), which in the case of N1 sample represents magnetically disordered atoms Fe^{3+}, and in the case of N2 sample Fe atoms belonging to $Fe_{2.x}N$ [8]. The Mössbauer spectrum of sample W1 contains three components: two doublets (*D1* and *D2*) which can be ascribed to wüstite in its nonstoichiometric form [9], and the third doublet (*D3*) representing Fe^{2+} ions in fayalite. For the last sample, C1, the spectrum is again composed of 7 components: one sextet (*S1*) represents α-Fe, two sextets (*S2* and *S3*) Fe atoms in nonstoichiometric magnetite, one sextet (S4) Fe atoms in iron carbide Fe_3C [10], two doublets (*D1* and *D2*) Fe^{2+} ions in nonstoichiometric wüstite, and last doublet (*D3*) Fe^{2+} ions in fayalite. Generally, the results of Mössbauer spectroscopy and XRD correlate well. The observed differences can be caused by presence of the low-crystalline to amorphous shell, which cannot be principally observed by XRD analysis.

The hysteresis loops measured at 300 K show the values of saturation magnetization for prepared materials (**Figure 1**). For sample W1 the hysteresis loop manifests the paramagnetic behavior of the material, which is for wüstite typical at room temperature. The magnetization of other samples is saturated at 5 T and reaches values 161.3, 93.9, and 102.6 Am^2/kg for samples N1, N2, and C1, respectively.

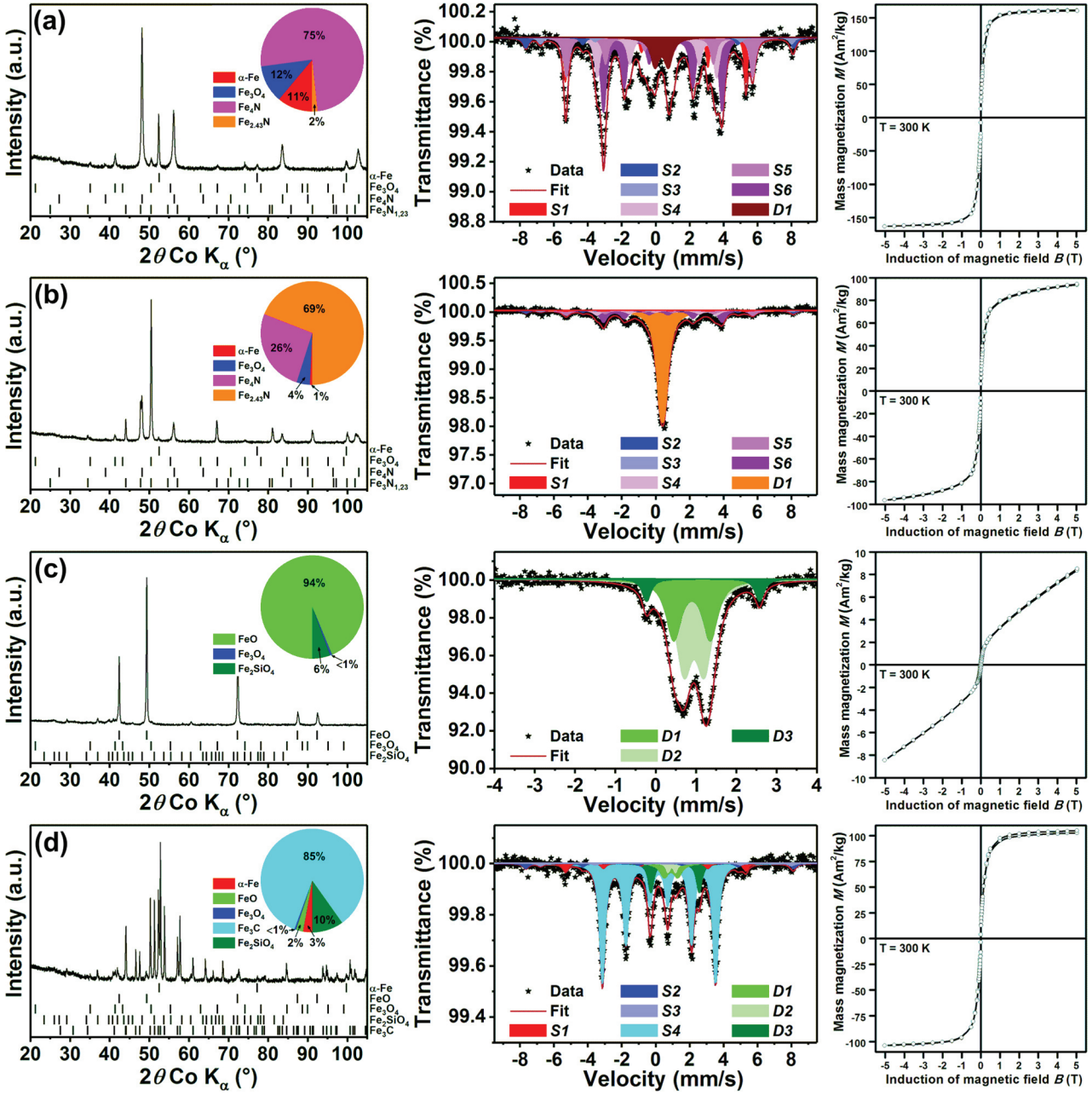

Figure 1 Diffraction patterns (left), Mössbauer spectra (middle), and hysteresis loops captured at 300 K (right) of prepared samples (a) N1, (b) N2, (c) W1, and (d) C1

3.2. Stability of prepared materials

The stability of prepared materials was evaluated after their exposure to the ambient atmosphere for 7 days. After their first contact with air, the materials evolved some heat as a result of their partial surface oxidation. Immediately performed structural and phase analysis (performed by XRD) revealed that the composition did not change significantly. However, the content of dominant phase decreased about approximately 2 or 3 wt% to the detriment of magnetite/maghemite. The additional storage did not initiate any further changes in composition of crystalline phases supporting the idea that the initial exothermic effect is a manifestation of creation of passivating shell on the surface of the particles.

Table 2 Hyperfine parameters of prepared samples derived from Mössbauer spectra. δ is the center shift, ΔE_Q is the quadrupole splitting, B_{hf} is hyperfine magnetic field, Γ is line width, and RA is relative subspectra area.

Sample	Component	δ ± 0.01 (mm/s)	ΔE_Q ± 0.01 (mm/s)	B_{hf} ± 0.3 (T)	Γ ± 0.01 (mm/s)	RA ± 1 (%)	Assignment
N1	*S1*	0.00	0.00	33.1	0.24	13	α-Fe
	S2	0.26	-0.04	49.1	0.38	5	^{tet}Fe (magnetite)
	S3	0.67	-0.11	46.0	0.38	3	^{oct}Fe (magnetite)
	S4	0.29	0.24	21.7	0.39	34	Fe_4N
	S5	0.22	0.00	34.1	0.38	18	Fe_4N
	S6	0.29	-0.45	21.9	0.38	18	Fe_4N
	D1	0.35	0.78	---	0.58	9	Fe^{3+}
N2	*S1*	0.00	0.00	33.0	0.33	1	α-Fe
	S2	0.26	-0.04	49.0	0.37	3	^{tet}Fe (magnetite)
	S3	0.67	-0.10	46.0	0.43	2	^{oct}Fe (magnetite)
	S4	0.29	0.24	21.7	0.50	18	Fe_4N
	S5	0.22	0.00	34.2	0.49	8	Fe_4N
	S6	0.29	-0.45	21.9	0.50	8	Fe_4N
	D1	0.39	0.26	---	0.58	60	$Fe_{2.x}N$
W1	*D1*	0.90	0.79	---	0.52	59	Fe^{2+} (wüstite)
	D2	0.95	0.44	---	0.45	33	Fe^{2+} (wüstite)
	D3	1.17	2.80	---	0.26	8	Fe^{2+} (Fayalite)
C1	*S1*	0.00	0.00	33.0	0.36	4	α-Fe
	S2	0.26	-0.04	49.1	0.38	3	^{tet}Fe (magnetite)
	S3	0.67	-0.11	46.0	0.38	2	^{oct}Fe (magnetite)
	S4	0.19	0.01	20.7	0.38	74	Fe_3C
	D1	0.90	0.79	---	0.58	6	Fe^{2+} (wustite)
	D2	0.95	0.44	---	0.26	2	Fe^{2+} (wustite)
	D3	1.14	2.84	---	0.36	9	Fe^{2+} (Fayalite)

3.3. Reactivity evaluation

The prepared materials were evaluated in terms of their efficiency towards Cr(VI) reduction (**Figure 2**). Moreover, their efficiency was comparable with unmodified nZVI (sample NF25). NF25 exhibited high removal efficiency, reaching 80 % of Cr(VI) removal after 48 hours. In comparison with that, the modified materials performed lower capacity but still adequate for such environmental applications. The most efficient were materials based on nitrides (i.e., the samples N1 and N2), which additionally contain a small residual portion of Fe^0. Their efficiencies were between 40 and 50 %. On the other hand, the material formed dominantly by wüstite (i.e., sample W1) exhibited relatively small efficiency, i.e., 15 % approximately. The iron carbide based material (sample C1) showed sufficient removal ability equal to 35 %.

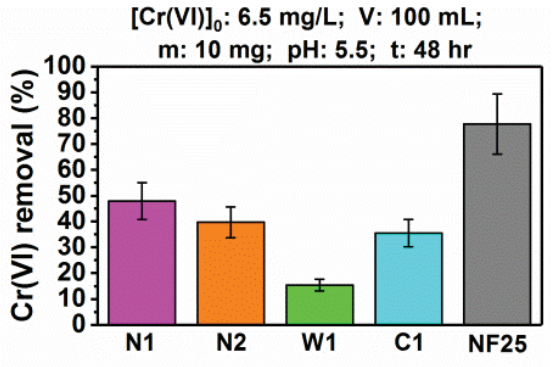

Figure 2 The efficiency of Cr(VI) removal by prepared materials after 48 hours

The mechanism of Cr(VI) removal was evaluated by XPS characterization of solid fractions obtained by filtering of the solution at the end of reactivity experiments. In all cases the Cr was identified only as Cr(III) without any traces of Cr(VI) (data not shown). Thus, the suggested removal mechanism involves reduction and subsequent precipitation of the reduced chromium species. It has to be mentioned, that the estimated lower removal capacity of the modified materials in comparison with the unmodified nZVI, is not a restrictive factor. In overall, these materials showed relatively high removal capacity reaching values of 35 mg of Cr(VI) per gram of material, values among the highest that involves nanoparticles for water remediation.

4. CONCLUSION

Four types of modification of bare nZVI were performed via one-step thermal treatment using different conditions. nZVI particles were modified in almost full volume of the particles rather than by only creation of a shell on the surface of the particles. Detailed structural and magnetic characterization revealed that each of the prepared materials is dominantly formed by different phase (i.e., by Fe_4N, $Fe_{2.43}N$, FeO, and Fe_3C). The prepared materials exhibited relatively high removal capacity which is comparable to conventional nanoparticles involved for water remediation. Moreover, these materials showed better stability and applicability in comparison to the bare nZVI, which is crucial for water treatment technologies.

ACKNOWLEDGEMENTS

The authors gratefully acknowledge support from project LO1305 of the Ministry of Education, Youth and Sports of the Czech Republic.

REFERENCES

[1] FU, F., DIONYSIOU, D.D. and LIU, H. The use of zero-valent iron for groundwater remediation and wastewater treatment: A review. *Journal of Hazardous Materials*. 2014. vol. 267, pp. 194-205.

[2] ZBORIL, R., ANDRLE, M., OPUSTIL, T., MACHALA, L., TUCEK, J., FILIP, J., MARUSAK, Z. and SHARMA, V.K. Treatment of chemical warfare agents by zero-valent iron nanoparticles and ferrate(VI)/(III) composite. *Journal of Hazardous Materials*. 2012. vol. 211, no. SI, pp.126-130.

[3] LI, X.-Q., ELLIOTT, D.W. and ZHANG, W.X. Zero-valent iron nanoparticles for abatement of environmental pollutants: materials and engineering aspects. *Critical Reviews in Solid State and Materials Sciences*. 2006. vol. 31, no. 4, pp. 111-122.

[4] KAŠLÍK, J., KOLAŘÍK, J., FILIP, J., MEDŘÍK, I., TOMANEC, O., PETR, M., MALINA, O., ZBOŘIL, R. and TRATNYEK, P.G. Nanoarchitecture of advanced core-shell zero-valent iron particles with controlled reactivity for contaminant removal. *Chemical Engineering Journal*. 2018. vol. 354, pp. 335-345.

[5] JOZWIAK, W.K., KACZMAREK, E., MANIECKI, T.P., IGNACZAK, W. and MANIUKIEWICZ, W. Reduction behavior of iron oxides in hydrogen and carbon monoxide atmospheres. *Applied Catalysis A: General*. 2007. vol. 326, no. 1, pp.17-27.

[6] GORSKI, C.A. and SCHERER, M.M. Determination of nanoparticulate magnetite stoichiometry by Mössbauer spectroscopy, acidic dissolution, and powder X-ray diffraction: A critical review. *American Mineralogist*. 2010. vol. 95, no. 7, pp. 1017-1026.

[7] BORSA, D.M. and BOERMA, D.O. Phase identification of iron nitrides and iron oxy-nitrides with Mössbauer spectroscopy. *Hyperfine Interactions*. 2003. vol. 151, no. 1, pp. 31-48.

[8] KSENOFONTOV, V., REIMAN, S., WALDECK, M. NEWA, R., KNIEP, R. and GUTLICH, P. In situ - High temperature Mossbauer spectroscopy of iron nitrides and nitridoferrates. *Zeitschrift Fur Anorganische Und Allgemeine Chemie*. 2003. vol. 629, no. 10, pp.1787-1794.

[9] CORNELL, R.M. and SCHWERTMANN, U. *The Iron Oxides: Structure, Properties, Reactions, Occurrences and Uses*. 2nd ed. Weinheim: WILEY-VCH Verlag GmbH & Co. KGaA. p. 664.

[10] BI, X.-X., GANGULY, B., HUFFMAN, G.P., HUGGINS, F.E., ENDO, M. and EKLUND, P.C. Nanocrystalline α-Fe, Fe_3C, and Fe_7C_3 produced by CO_2 laser pyrolysis. *Journal of Materials Research*. 1993. vol. 8, no. 7, pp.1666-1674.